International Research Journal of Engineering and Technology (IRJET) e-ISSN: 2395-0056
Volume: 06 Issue: 02 | Feb 2019 www.irjet.net p-ISSN: 2395-0072

Finite Element Analysis of a Leading edge Flutter Wind Energy Generator

Nagaraj V [1], Arun negemiya A[2], Karthic Subramaniyan I[3], Udhay Sankar R[4]

[1]Asst. Prof. Aerospace Dept.,& Periyar Maniammai Institute of Science and Technology, Periyar Nagar, Vallam, Thanjavur, Tamil Nadu, India- 613403
[2]Research Scholar, Centre for Materials Joining and Research (CEMAJOR), Department of Manufacturing Engineering, Annamalai University, Chidambaram – 608002, Tamil Nadu, India
[3]Asst. Prof. Aerospace Dept., & Periyar Maniammai Institute of Science and Technology, Periyar Nagar, Vallam, Thanjavur, Tamil Nadu, India - 613403
[4]Asst. Prof. Mechanical Dept.,& Periyar Maniammai Institute of Science and Technology, Periyar Nagar, Vallam, Thanjavur, Tamil Nadu, India – 613403

Abstract - *Aeroelastic wind energy generator which produces the high power in low air velocity using one of the aeroelasticity dynamic instability phenomenon called flutter (self-exciting oscillation). The proper controlled aerodynamic flutter phenomenon is used positively in this project for produce the power (generating the electricity). A model of an aeroelastic wind energy generator machine is developed and its performance under various conditions is discussed. The idea of utilizing wind power to extract energy is not new. However, there is a recent interest in the energy extraction from the torsional flutter of a rigid airfoil with near stalling angle of attack. The restoring force is generated by the use of a torsional spring. The mathematical analyses are used to predict the model optimum geometry, flutter speed, and frequency. Damping oscillation, practical resonance, and transient oscillation solution are developed. Numerical treatment has been carried out to the prediction of the parameters influence in design. The solutions were validated with reference and significant influencing parameters were found.*

Key Words: Aeroelasticity, Flutter, Wind Energy.

1. INTRODUCTION

The studies of the unsteady flows past oscillating aerofoils have been mostly motivated by the efforts made to avoid or reduce undesirable unsteady effects in aeronautics, such as flutter, buffeting and dynamic stall [1-2]. The unsteady aerodynamic force acting on the oscillating aerofoil has one degree of freedoms and Aeroelastic characteristics of oscillating aerofoil have been determined by an unsteady small disturbance theory which is used to more effectively analyze the unsteady aerodynamic oscillating aerofoil [3-5]. The solution of fluid-structure interaction problems coupling computational fluid dynamics (CFD) analysis with transient structural response analysis is now becoming tractable through the accessibility of high-performance computing [6-7]. Aeroelasticity is the multidisciplinary science dealing with the interaction of aerodynamic forces and structural deformations. As the structure moves through the air, the motion will cause aerodynamic loads, leading to deformation of the structure. The deformation, in turn, has an impact on the airflow, thus changing the aerodynamic loading. Apparently, there is a closed loop of aerodynamic and structural interactions depending on the properties of the structure and the airflow which will cause different aeroelastic phenomena. Aeroelastic phenomena can be divided into different groups depending upon the participation of specific members of the fluid-structure system. The aeroelastic system properties consist of three major components: aerodynamic forces due to the motion of the structure in the air, elastic and inertial forces due to the structural deformation and acceleration.

The problems of flutter of airplane wings and suspension bridges are among the well-studied subjects in the field of aeronautical engineering [8-10]. The cause of the flutter of airplane wings or suspension bridges, very crudely, may be explained as an aeroelastic coupling where the energy is transferred from the air stream into the elastic structure and hence a destructive, monotonically increasing amplitude of the vibration of the structure results. In other words, the vibration of the elastic structure becomes negatively damped, and therefore the amplitude of the vibration increases until the structure fails. The failure of the Tacoma Narrows Bridge is one of the well-known examples of such disasters. Therefore, it appears that aeroelastic instability or flutter could be a method for converting wind energy into mechanical energy [11-13]. An airplane wing or a suspension bridge must be designed so that they are aero elastically stable since in the flutter state the transferred wind energy is stored as elastic strain energy and an ever-increasing amplitude of the vibration of the structure follows. Now, if a structure were constructed such that in the flutter state the transferred wind energy could be extracted from it, such a structure could become a wind energy converter.

The aim of this work is to present computational solutions for unsteady compressible flows past rigid aerofoil executing

low-frequency oscillations. These efficient computational solutions are obtained by ANSYS WORKBENCH.

2 THEORETICAL BACKGROUND

2.1 Modelling of fluid-structure interaction

The physical models used in treating fluid-structure interaction phenomena vary enormously in their complexity and range of applicability. The simplest model is the very popular "piston theory", which may be thought of as the limit of potential-flow models as the frequency of an oscillating body in a fluid becomes large [14-16]. It also may be thought of like the double limit as the Mach number becomes large, but the product of the Mach number and amplitude of oscillation normalized by body chord remains small compared with unity. This simplest theory expresses the fluid pressure p on the oscillating body at some point x, y, and sometimes t as a simple linear function of the motion at that same point and instant in time. That is,

$$p = (\rho U/M)\left[\frac{\partial w}{\partial t} + U\frac{\partial w}{\partial x}\right]$$

Where w is a function of x, y, and t and is the instantaneous deflection of the body in the fluid stream, p, U, and M are the free-stream density, velocity, and Mach number, respectively. This simple fluid mechanics model has been very popular with structural engineers because it allows the fluid pressure to be incorporated into a standard structural dynamic with a minimum of additional complexity. But this fluid model is physically useful over only a limited range of flow conditions, and its primary value is in checking the results from more complex fluid models in the appropriate limit. There is a nonlinear version of the piston theory, but it still is limited in the frequency or Mach number range where it is useful. Small-perturbation form of the potential-flow theory that leads to the celebrated linear converted wave equation for the velocity potential Φ; that is,

$$\nabla^2\phi - \frac{D^2\phi}{Dt^2} = 0$$

where ∇ϕ is the Laplacian operation and D/Dt is the substantial derivative, which is, in turn,

$$\frac{D}{Dt} \equiv \frac{\partial}{\partial t} + U\frac{\partial}{\partial x}$$

The solution of the linear converted-wave equation forms the basis for many of the fluid-structure interaction models that have been used for fluid-structure interaction stability and response analyses of aircraft. These are termed "flutter" or "gust response" analyses.

2.2 The computational challenge of fluid-structure interaction modeling

The fluid-structure interaction analyst has a special challenge. If one wished to obtain solutions for many different combinations of structural and fluid parameters, then the solutions to the CFD and other fluid models must be made as computationally efficient as possible. Typically, a design team may wish to evaluate thousands of parameter variations as various structural elements are changed in the design process. For many years, in the analysis of complex structures, the finite-element model for a structural body undergoing oscillations has been "reduced" in size by first finding the natural or Eigenmodes of the structure and then recasting the finite-element structural model in terms of these modes, using, for example, Lagrange's equations from classical dynamics. Typically, a finite-element structural model of a few thousand degrees of freedom has been reduced to a modal model with a few tens of degrees of freedom.

An oscillating aerofoil to demonstrate set up and run a simulation involving two-way Fluid-Structure Interaction (FSI) in ANSYS Workbench. The structural physics is set up in the Transient Structural analysis system and the fluid physics is set up in Fluid Flow (CFX) analysis system, but both structural and fluid physics are solved together under the Solution cell of the Fluid system. Coupling between two analysis systems is required throughout the solution to model the interaction between structural and fluid systems as time progresses. The framework for the coupling is provided by the ANSYS Multi-field solver using the MFX setup. When ANSYS CFD-Post reads an ANSYS results file, all the ANSYS variables are available to plot on the solid, including stresses and strains. The mesh regions available for plots by default are limited to the full boundary of the solid, plus certain named regions which are automatically created when particular types of load are added in Simulation. For example, any Fluid-Solid Interface will have a corresponding mesh region with a name such as FSIN 1. In this case, there is also a named region corresponding to the location of the fixed support, but in general pressure, loads do not result in a named region.

2.3 Problem analysis

There are three variables in wing flutter

1. Flexure Flutter
2. Torsion Flutter
3. Control surface rotation.

The rigid airfoil so constrained as to have only the flexural degree of freedom does not flutter. A rigid airfoil with only the torsional degree of freedom can flutter only if the angle of attack (AOA) is at or near the stalling angle. So, consider

the oscillation of aileron control in the wing. That is control surface rotation of rigid aerofoil.

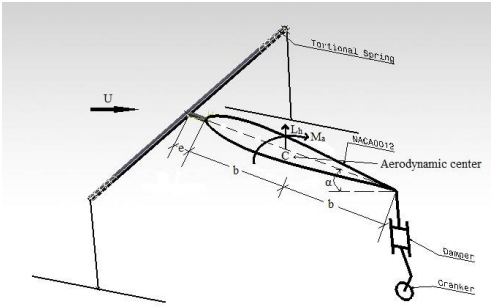

Figure1 Model of the leading-edge flutter wind energy generator

Consider only rigid wing with span Ls. Rotates about leading edge with an only torsional degree of freedom does not have flexure flutter. Figure 1 shows the symmetric AerofoilNACA 0012, a Chord length of the aerofoil 2b. Lift and moment of the wind areLh and Ma.

Derivation of equation of motion of the system

$$I\alpha(d2\alpha/dt2) + k\,\alpha\alpha = ML \quad (1)$$

Where

Ma - Moment about leading edge of the aerofoil.

Iα- Moment of inertia about the leading edge.

α- Angle of the restrained position of the wing.

k α- torsional stiffness of the spring.

Lh- Total aerodynamic lift of the moving blade airfoil, at the mid-chord point C.

b - Half-width of the blade airfoil.

e - Horizontal axis eccentricity from structural support.

C - Midpoint, mid-chord.

Equation 1 become

$$I\alpha[\,(d2\alpha/dt2)+w\,\alpha2\alpha] = ML \quad (2)$$

Where,

w α - frequency of oscillation of the wing

$$w\,\alpha2 = k\,\alpha\,/\,I\alpha$$

Where t and w α are dimensional variable,

Let us introduced following dimensionless variable Dimensionless time

$$S = (t\,U)/b$$

Dimensionless frequency (Reduced frequency or strouhal number)

$$k = (w\,\alpha\,b)/\,U$$

Equation 2 becomes

$$[\,(d2\alpha/ds2)+k2\alpha] = (b2\,/U\,I\alpha)\,ML\,(s) \quad (3)$$

Where, ML (s) – unsteady aerodynamic moment

Unsteady aerodynamic moment is solved by using thin airfoil oscillating in incompressible flow and theodorsen method.

Unsteady aerodynamic moment:

$$ML\,(s) = \Pi\rho\ b2\ U2\ L(-((1.5d\alpha/ds)+(1.125\ d2\alpha/ds2))-(\alpha+1.5d\alpha/ds)c(k)) \quad (4)$$

Substituting equation 4 into equation 3

$$d2\alpha/ds2(1+1.125e)+ d\alpha/ds(1.5e(1+c(k))+ \alpha(k2+ec(k))=0 \quad (5)$$

Where,

$$e = (\Pi\rho\ b4\ U2L)/\,I\alpha$$

e - Generalized inertia parameter.

C (k)- it is the ratio the quasi-steady flow into the quasi-unsteady flow.

It's called Theodorsen function.

Equation 5 is the equation of motion of the system.

Generalized inertia parameter

$$e = (\Pi\rho\ b4\ U2L)/\,I\alpha$$

$$102 < I\alpha/\,L < 106 \quad kg\ m2/m$$

3. EXPERIMENTAL WORK

The NACA 0012, the well-documentedaerofoil from the 4-digit series of NACA airfoils, was utilized. Table 1 shows the NACA 0012 Airfoil coordinates.The NACA 0012 aerofoilis symmetrical; the 00 indicates that it has no camber. The 12 indicates that the airfoil has a 12% thickness to chord length ratio; it is 12% as thick as it is long. Figure 2 shows NACA 0012 Aerofoil. Reynolds number for the simulations was Re=3x106. The free stream temperature is 300 K, which is the same as the environmental temperature. The density of the

air at the given temperature is ρ=1.225kg/m3 and the viscosity is μ=1.7894×10-5kg/ms. For this Reynolds number, the flow can be described as incompressible. This is an assumption close to reality and it is not necessary to resolve the energy equation. A segregated, implicit solver was utilized (ANSYS FLUENT 14.0) Calculations were done for angles of attack ranging from 0° to 10°. The aerofoil profile, boundary conditions, and meshes were all created in the ANSYS FLUENT. The resolution of the mesh was greater in regions where greater computational accuracy was needed, such as the region close to the airfoil. The first step in performing a CFD simulation should be to investigate the effect of the mesh size on the solution results [17-18]. Generally, a numerical solution becomes more accurate as more nodes are used, but using additional nodes also increases the required computer memory and computational time. The appropriate number of nodes can be determined by increasing the number of nodes until the mesh is sufficiently fine so that further refinement does not change the results. Figures 3 and 4 show that design geometry and CATIA model.

Table 1 NACA 0012 Aerofoil coordinates

NACA 0012			
UPPER SURFACE		LOWER SURFACE	
x/c	y/c	x/c	y/c
1	0.00126	0	0
0.997261	0.001644	0.002739	-0.00911
0.989074	0.002783	0.010926	-0.01777
0.975528	0.004642	0.024472	-0.02589
0.956773	0.007168	0.043227	-0.03339
0.933013	0.010286	0.066987	-0.04015
0.904508	0.013914	0.095492	-0.04605
0.871572	0.017959	0.128428	-0.051
0.834565	0.022323	0.165435	-0.0549
0.793893	0.026905	0.206107	-0.05771
0.75	0.031603	0.25	-0.05941
0.703368	0.036311	0.296632	-0.06002
0.654508	0.040917	0.345492	-0.05958
0.603956	0.045307	0.396044	-0.05818
0.552264	0.049358	0.447736	-0.05592
0.5	0.05294	0.5	-0.05294
0.447736	0.055923	0.552264	-0.04936
0.396044	0.058175	0.603956	-0.04531
0.345492	0.059575	0.654508	-0.04092
0.296632	0.060015	0.703368	-0.03631
0.25	0.059412	0.75	-0.0316
0.206107	0.057714	0.793893	-0.02691
0.165435	0.054902	0.834565	-0.02232
0.128428	0.050996	0.871572	-0.01796
0.095492	0.046049	0.904508	-0.01391
0.066987	0.040145	0.933013	-0.01029
0.043227	0.033389	0.956773	-0.00717
0.024472	0.025893	0.975528	-0.00464
0.010926	0.01777	0.989074	-0.00278
0.002739	0.009114	0.997261	-0.00164
0	0	1	-0.00126

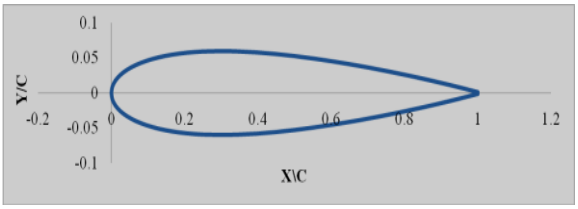

Figure 2 NACA 0012 Aerofoil

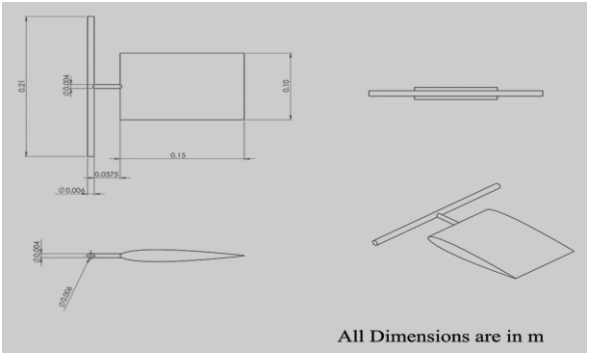

Figure 3 Design parameters

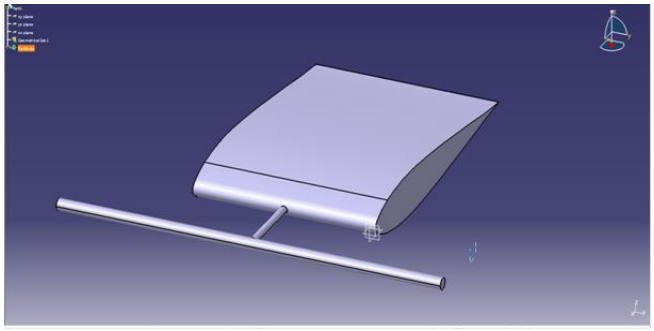

Figure 4 CATIA model

4. COMPUTATIONAL ANALYSIS

4.1 Ansys

ANSYS, Inc. is an engineering simulation software (computer-aided engineering, or CAE) developer that is headquartered south of Pittsburgh in Canonsburg, Pennsylvania, United States. ANSYS was listed on the NASDAQ stock exchange in 1996. In late 2011, Investor's Business Daily ranked ANSYS as one of only six technology businesses worldwide to receive the highest possible score on its Smart Select Composite Ratings. ANSYS has been recognized as a strong performer by a number of other sources as well. The organization reinvests 15 percent of its revenues each year into research to continually refine the software.

4.2 Boundary Conditions

The boundary conditions given in the gambit were maintained and the input values were given. These values are given in Table 2 below.

Table 2 Boundary Condition

Variables	Engine with a single nozzle	Engine with multiple nozzles
Velocity (m\s)	200,225,250	200,225,250
Total Pressure (Po) in Pascal	0.912 x 105	0.912 x 105
Density (ρ) in kg/m3	0.98	0.98
Temperature in K	900	900

4.3 CFD analysis for airfoil

The CFD Results has been carried out for Streamline, Pressure and Velocity contours and the graphs corresponding to the parameters [19]. Figure 5 shows the streamline flow at a various angle of attack

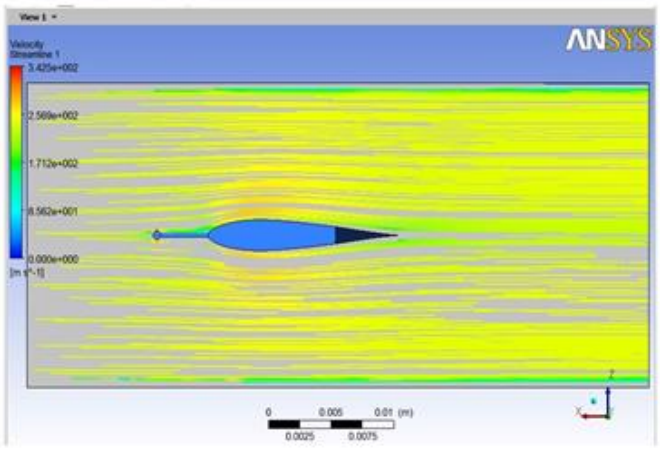

(a) 0°

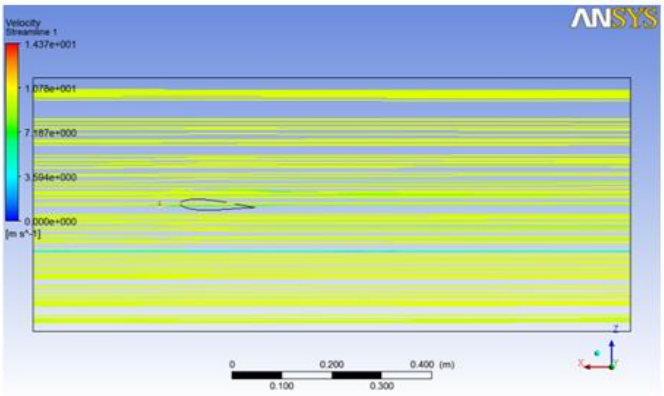

(b) 3°

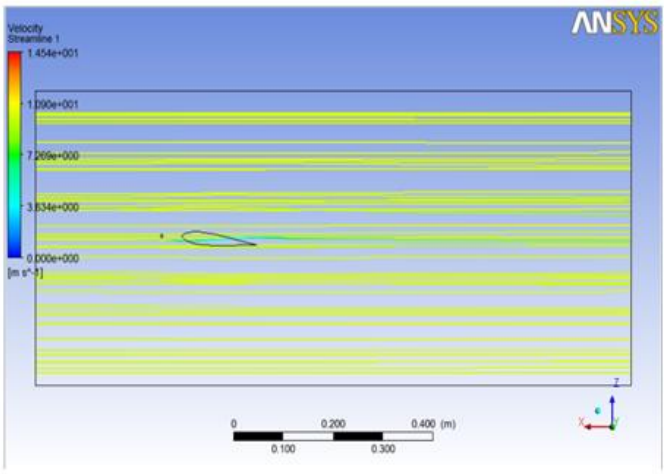

(b) 6°

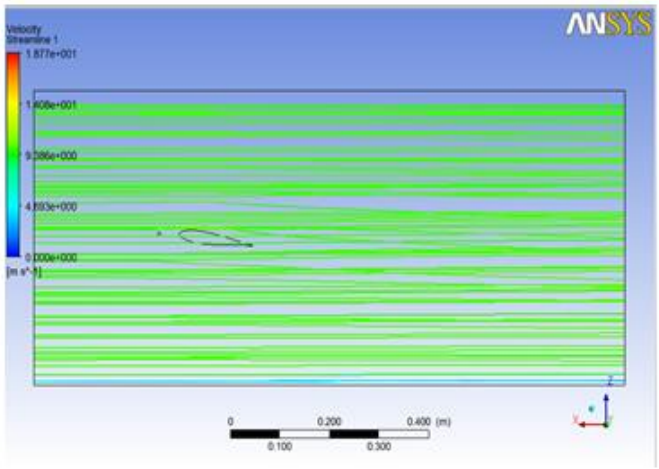

(c) 8°

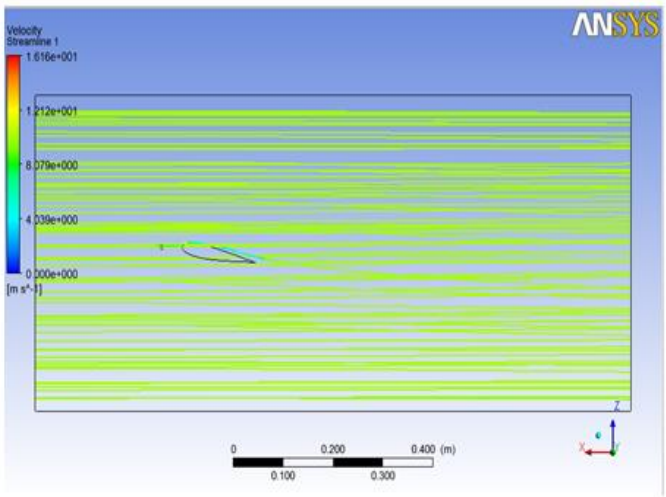

(e) 10°

Figure 5 Streamline flow at various AOA

4.4 Pressure distribution

The pressure distribution is the contour which shows the distribution of pressure in and around the object to clearly visualize the performance prediction. Figures 6 shows the pressure distribution over the airfoil when it is operated with one outlet conditions. Then the airfoil is analyzed for different inlet velocities [20].

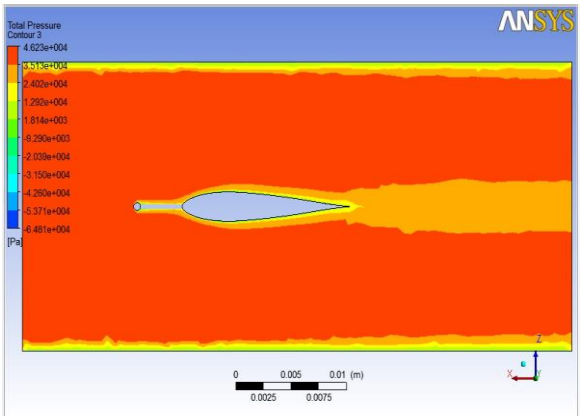

(a) 0°

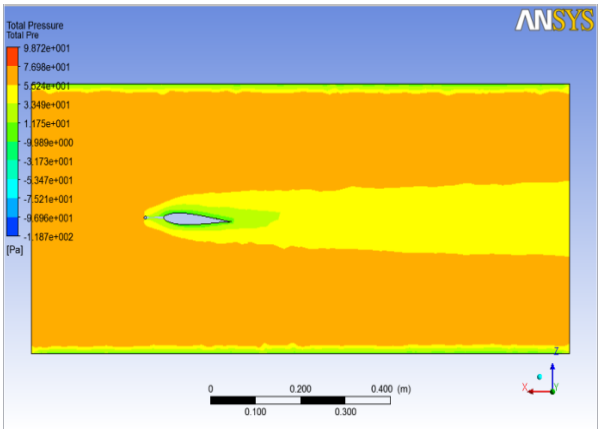

(b) 3°

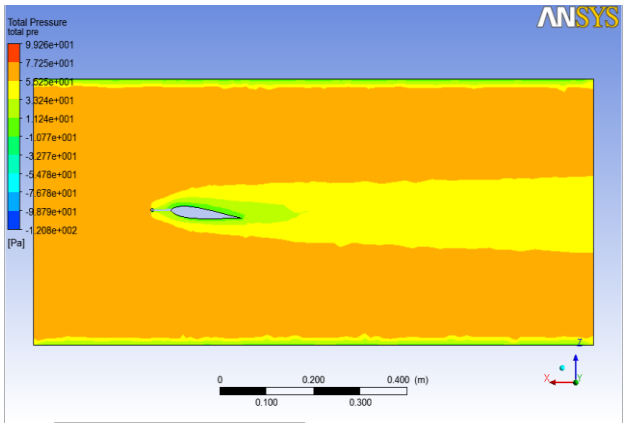

(c) 6°

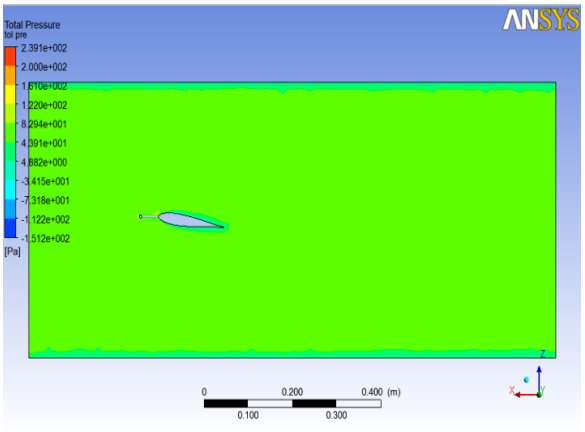

(d) 8°

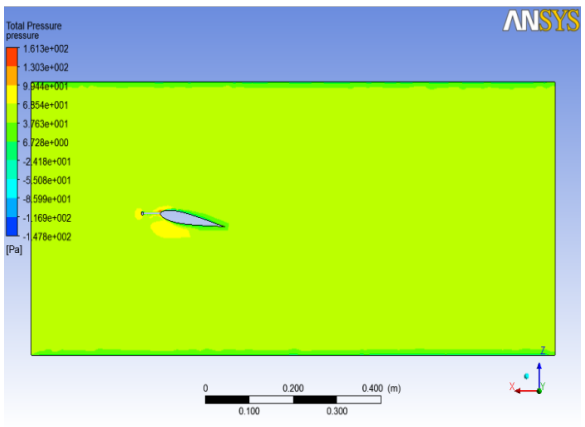

(e) 10°

Figure 6 Pressure contour at various AOA

4.5 Velocity distribution

Velocity Distribution diagram is a diagram which shows the distribution of velocity over the upper and lower parts of the airfoil which is in the flow field. Figures 7 shows the velocity distribution over the airfoil when it is operated with one outlet conditions

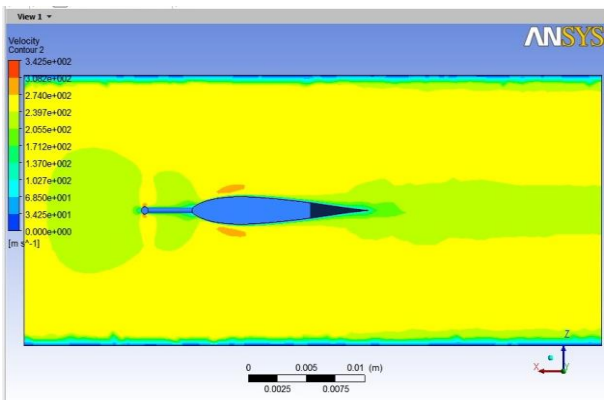

(a) 0°

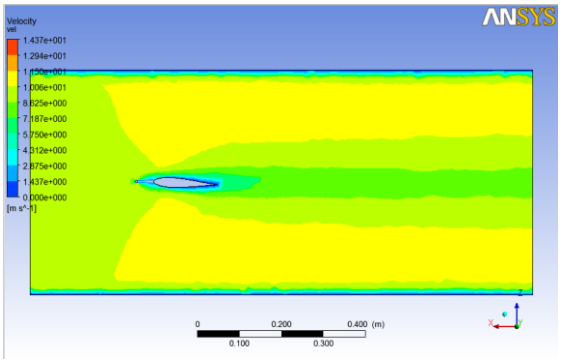

(b) 3°

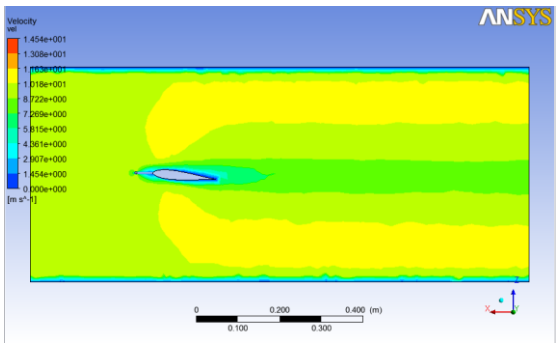

(c) 6°

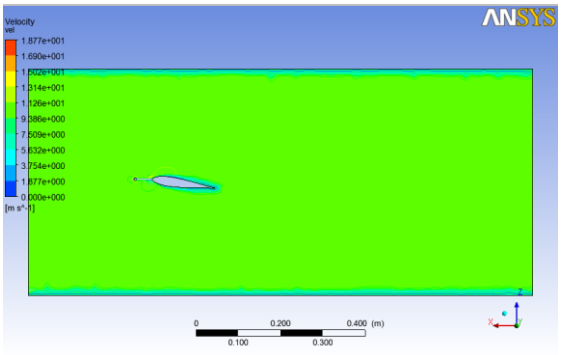

(d) 8°

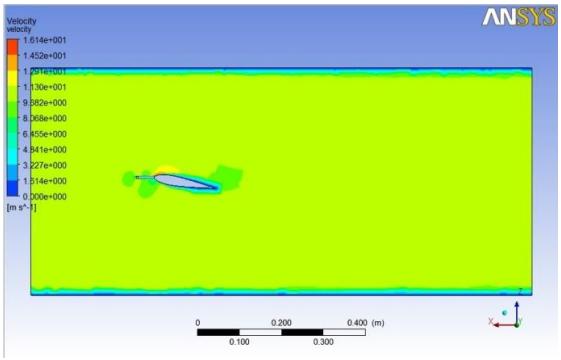

(e) 10°

Figure 7 Velocity contour at various AOA

4.6 Mesh file

Figure 8 shows the drawing of the airfoil which is drawn in ANSYS FLUENT. In this software, a key point has to be created and the lines are drawn then the line has been created. Then for analyzing purpose, the lines have to be faced. Then the messing operation is done for calculating the best performance of the airfoil. The Tetrahedral mesh has been the mesh has created in a minute manner for better accuracy carried out for this purpose of analysis and the accuracy will depend on the type of meshing and the smoothness of the mesh.

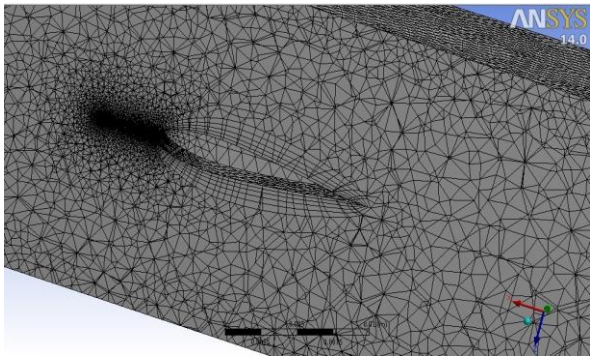

Figure 8 Tetrahedral meshing

5. RESULTS AND DISCUSSION

The model is designed in CATIA and analyzed in ANSYS WORKBENCH. The oscillator model is designed based on the four incident variations, respectively 3, 6, 8, 10 degrees. The comparison curve for pressure distribution (Table 3) of the oscillation Figure 9 is given below.

Table 3 Pressure variations with respect to the angle of attack

Angleof attack (deg)	Max pressure (Pa)	Min pressure (Pa)
3	70.2	34.9
6	22.2	-10.8
8	61	21.7
10	59.6	20.9

The displacement at a various angle of attack (Table 4) are compared by the curve Figure is given below. Figure 10 shows that up to 8° the displacement increases continuously, but at 10° the stall occurs suddenly and the displacement reduces. It is concluded that the angle of incidence should not be more than 8°.

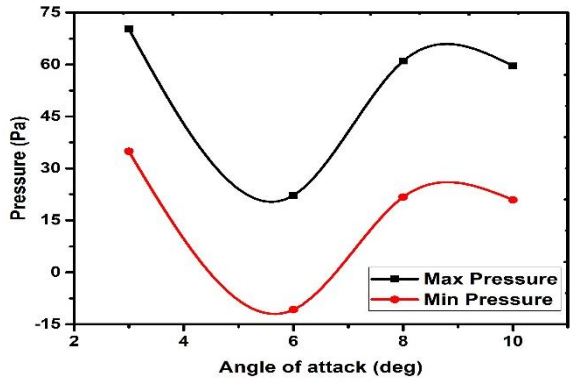

Figure 9 Pressure vs. angle of attack

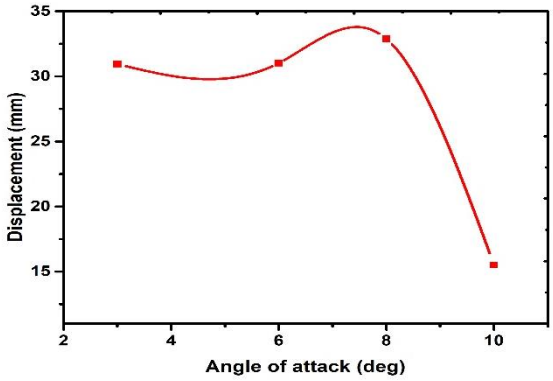

Figure 10 Displacement vs. angle of attack

Table 4 Variation of displacement with respect to the angle of attack

Angleof attack (deg)	Frequency (Hz)	Displacement (mm)	Displacement in RPM
3	3.41	30.96	204.6
6	4.67	31.02	280.2
8	4.7	32.89	282
10	4.72	15.5	283.2

Table 5 Variation of CL and CD with respect to the angle of attack

Angleof attack (deg)	CL	CD
3	0.0021	-1.472
6	0.0101	-1.484
8	0.0105	-1.542
10	-0.0076	-1.566

Table 6 Variation of CP, velocity, and power with respect to the angle of attack

Angleof attack (deg)	CP	Power (Watt)	Velocity (m/s)
3	0.187	11.15	5.75
6	0.181	11.25	5.81
8	0.0671	166.41	13.14
10	0.0495	205.92	11.31

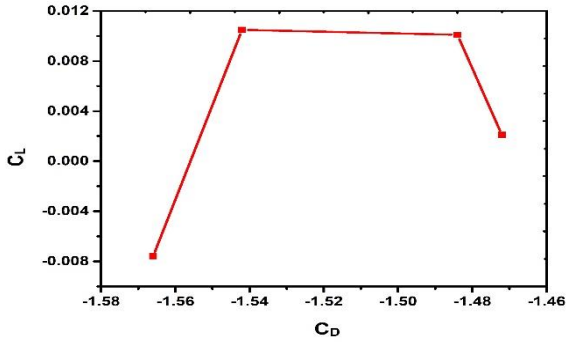

Figure11 CL vs. CD

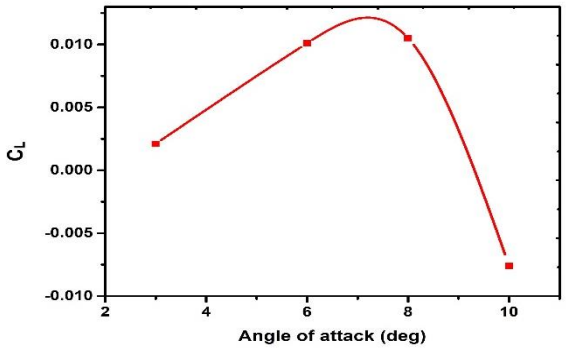

Figure12 CL vs. angle of attack

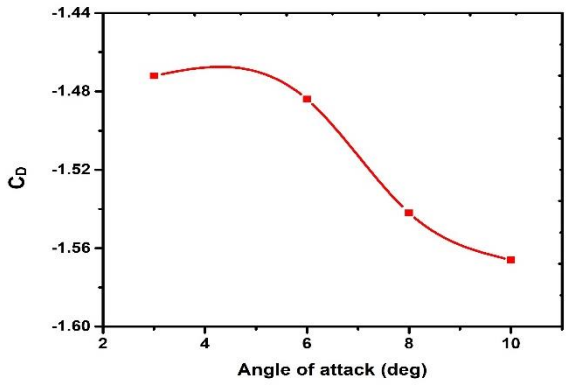

Figure13 CD vs. angle of attack

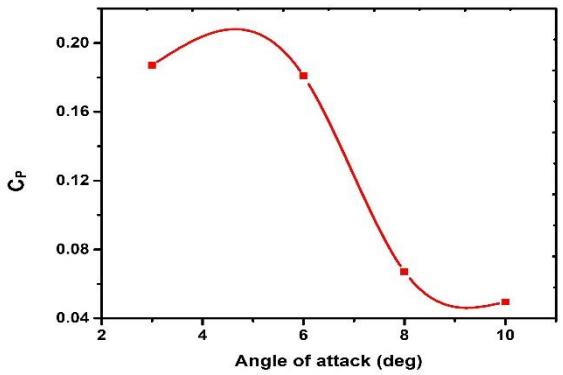

Figure14 CP vs. angle of attack

Figure 11 illustrates that CL vs. CD graph and values were taken from Table 5. Figure12 shows that till 8° the lift is maximum and when the angle of attack is further increased stall occurs and CL decreases. Figure 13 shows that CD increases when the stalling angle occurs. Table 6 shows that CP gradually increases with velocity and there is a power drop. Figure 14 shows that angles of attack increased and CP values are decreased.

Equation of power coefficient

CP = ½ [1-(V22/V12)]*(V2/V1)

P total = ½ g (ρAVi3)

P max = CP * Ptotal

Where,

CP - Power coefficient.

A - Frontal area of the rectangular wing.

ρ - Density of air.

g - Gravitational force.

V1 - Velocity at the leading edge.

V2 - Velocity at trailing edge.

6. CONCLUSIONS

The computational rigid aerofoil model with a torsional degree of freedom is created using CATIA software.

The static structural and fluid flow analyses carried out using ANSYS software at various angles of attack of 3, 6, 8, 10. For the natural air velocity condition is 10m/s.

The pressure distribution curve for various angles of attack shown the stalling angle of the oscillator. It is found that a phenomenon called flutter occurs at high angles of attack or nearly stalling angle. Also, there is an increase in aerodynamic loading on the system again confirms the occurrence of flutter.

Displacement and angle of attack curve shown the maximum displacement occurred at 8° angle of attack. It is concluded that the oscillator angle should not more than 8° for the maximum power output.

REFERENCES

[1] Adnan Harb, Energy harvesting: state of the art, J. Renewable Energy, 2011.

[2] N.G.Stephen, on energy harvesting from ambient vibration, J. Sound Vib., 2006.

[3] Bisplinghoff, R.L., Ashley, H., Halfman, R.L., Aeroelasticity. Dover Publications Inc., Mineola, NY, USA, 1955.

[4] D. Poirel, Y. Harris, A. Benaissa, Self-sustained aeroelastic oscillations of a NACA0012 airfoil at low-to-moderate Reynolds numbers, J. Fluids Struct. vol. 24. pp. 700–719, 2008.

[5] Fung, Y.C., An Introduction to the Theory of Aeroelasticity. Dover Publications, New York, 1969.

[6] WANG.ye-wei, Ling yong-wen, Combination of CFD & CSD packages for fluid structure interaction, J. hydrodyn. 2008.

[7] Ramji Kamakoti, Wei shyy, Fluid-Structure interaction for aeroelastic applications, 2005.

[8] Luca Caracoglia, Feasibility assessment of a leading-edge-flutter wind power generator, J. Wind Eng.Ind. Aerodyn.;98:679-686, 2010.

[9] Theodore Theodorsen, General Theory of Aerodynamic Instability and the Mechanism of Flutter. NASA Technical Report no.496, 1935.

[10] Dang Huixue, Yang Zhichun, Li Yi, Accelerated loosely coupled aeroelastic model for nonlinear static aeroelastic analysis, 2008.

[11] W.A.Silva, R.E.Bartels, Development of reduced-order model for aeroelastic analysis and flutter prediction using CFL3DV6.0 code, 2009.

[12] G.S.L.Goura, K.J.Badcock, M.A.Woodgate, B.E.Richards, A data exchange method for Fluid-Structure interaction problems, 2001.

[13] Charles M. Hoke, Comparison of Overset Grid and Grid Deformation Techniques Applied to 2-Dimensional NACA Airfoils, 19th AIAA Computational Fluid Dynamics Conference, 2009.

[14] Goodarz, A., Aeroelasticity wind energy converter. Journal of Energy Conversion, 1978.

[15] Ira H. Abbott, Theory of wing sections. Dover Publications, Inc. New York, 1959.

[16] B. H. K. Lee, L. Gong,and Y. S. Wong, Analysis and computation of nonlinear dynamic response of a two-degree-of-freedom System and its application in aeroelasticity". J. Fluids Struct. vol. 11. pp. 225 – 246, 1997.

[17] D. Poirel, W.Yuan, Aerodynamics of laminar separation flutter at a transitional Reynolds number, J.Fluids Struct. 2010.

[18] Udbhav Sharma, Effects of Airfoil Geometry and Mechanical Characteristics on the Onset of Flutter, School of Aerospace Engineering Georgia Institute of Technology December 10, 2004.

[19] Wang.D.A, K.H.Chang, Electromagnetic energy harvesting from flow induced vibration. Microelectron. J vol.41. pp. 356–364, 2010.

[20] Douvi C. Eleni, tsavalosI.Athanasios and MargarisP.Dionissios, Evaluation of turbulence models for the simulation of flow over a NACA 0012 airfoil, 2012.